Oxygen concentration and modeling thermal decomposition of a high-performance material: A case study of polyimide (Cirlex)

Aditya Ramgobin, Gaelle Fontaine, Serge Bourbigot

Oxygen Concentration and Modeling Thermal Decomposition of a High-Performance Material: A Case Study of Polyimide (Cirlex)

Aditya Ramgobin [1], Gaëlle Fontaine [2] and Serge Bourbigot [2]*

[1] Univ. Lille, CNRS, INRAE, Centrale Lille, UMR 8207 - UMET - Unité Matériaux et Transformations, F-59000 Lille, France, aditya.ramgobin@univ-lille.fr,

[2] Univ. Lille, CNRS, INRAE, Centrale Lille, UMR 8207 - UMET - Unité Matériaux et Transformations, F-59000 Lille, France, gaelle.fontaine@ensc-lille.fr

* Correspondence: serge.bourbigot@ensc-lille.fr

Abstract: Kinetic decomposition models for the thermal decomposition of a high-performance polymeric material (Polyimide, PI) were determined from specific techniques. Experimental data from thermogravimetric analysis (TGA) and previously elucidated decomposition mechanism were combined with numerical simulating tool to establish a comprehensive kinetic model for the decomposition of PI under three atmospheres: nitrogen, 2% oxygen, and synthetic air. Multi-staged kinetic models with subsequent and competitive reactions were established by taking into consideration the different types of reactions that may be occurring during the thermal decomposition of the material (chain scission, thermo-oxidation, char formation). The decomposition products and decomposition mechanism of PI which was established in our previous report allowed for the elucidation of the kinetic decomposition models. A three-staged kinetic thermal decomposition pathway was a good fit to model the thermal decomposition of PI under nitrogen. The kinetic model involved an autocatalytic type of reaction followed by successive nth order reactions. Such types of models were set up for the evaluation of the kinetics of the thermal decomposition of PI under 2% oxygen and in air, leading to models with satisfactory fidelity.

Keywords: kinetic analysis, polymer decomposition, high performance polymers, simulation

1. Introduction

Polyimide (Cirlex or Kapton, PI) is a high-performance polymeric material used in a wide array of applications, due to its outstanding physical properties. Indeed, polyimides are known to have exceptional thermal stability. This is attributed to their rigid heterocyclic imide and aromatic rings on the polymer backbone[1]. They are used in fields such as microelectronics, high temperature matrices, as well as for gas separation membranes.

Previous work on the thermal stability and decomposition of polyimide has been performed at our laboratory[2], whereby different behavioral traits of PI were investigated. These traits involved the investigation of the thermal decomposition mechanism under pyrolytic conditions, the incidence of oxygen concentration on the thermal stability of PI, as well as the evaluation of the fire behavior of PI under different heat fluxes using the mass loss cone calorimeter.

In our previous work, we have evidenced that the thermal behavior of PI is quite different depending on the oxygen concentration. There are several stages involved in the thermal decomposition of PI, and the stages differ greatly whether the thermal stress is oxygen rich or deprived. Therefore, in order to complement the thermal decomposition of PEEK in a fire scenario, kinetic models corresponding the decomposition in oxygen-free, oxygen-poor, and oxygen rich (air) atmosphere need to be investigated.

The TG and DTG plots of thermogravimetric analysis (TGA) performed on PI at different oxygen concentrations (**Figure 1**) show that the initial degradation temperature is not highly dependent on the oxygen concentration. However, it is clear from the TG plots that at high temperatures, the role of oxygen in the thermal decomposition of PI is significant. Indeed, at higher temperatures (above 600 °C), the mass loss increases with increasing oxygen concentration. This suggests that the thermal decomposition mechanism is also highly dependent on the oxygen concentration, even if it is as low as 2%.

Figure 1. TG and DTG plots of PI heated at 10 °C/min under nitrogen, 2%, 4%, 8% and 12%, and in air[2].

In order to further the understanding of the thermal decomposition characteristics of PI, it was undeniably important to evaluate the kinetic parameters that govern its thermal decomposition. In our previous work, we have observed that the presence of oxygen may impact both the onset of the thermal decomposition and the char degradation process[2].

Different oxygen concentrations correspond to different parts of a fire scenario. Indeed, a material under a flame is scarcely in contact with oxygen because the flame usually consumes all the oxygen in the surrounding environment. Therefore, the decomposition behavior at this point corresponds to solely pyrolytic effects.

However, if there is the presence of only a small flame, there may be some oxygen (much lowered concentration as compared to air, as low as 2%) that is in contact with the material. Furthermore, if the material is found away from a flame in a well-ventilated environment, it subjected to thermal stress in the presence of air. Thus, modelling the three oxygen levels may provide an integral insight on the decomposition behavior of a burning material.

Therefore, it was of interest to evaluate the kinetic parameters of the thermal decomposition of the material under three different oxygen concentrations: 0%, 2%, and 20% (synthetic air).

2. Materials and Methods

Polyimide (Cirlex CL) was purchased from Goodfellow Cambridge Limited (Huntington, England)

2.1. Thermogravimetric Analysis (TGA)

Thermogravimetric analyses (TGA) were conducted on a Netzsch Libra instrument. Powdered samples of 9 - 10 mg (according to the good practice of TGA, it is assumed the samples are thermally thin) were placed in open alumina pans and heated up to 900 °C under different percentages of oxygen and nitrogen at different heating rates (1, 2, 5, and 10 °C/min) up to 900 °C under 0%, 2%, and 20 % oxygen concentrations.

2.2. Kinetic Analysis

Kinetic analysis and modeling of the degradation of the samples were made using a Kinetics Neo software package developed by Netzsch Company. The principle has been discussed by Opfermann in[3] and here we only briefly remind the reader of the basic concepts of the method.

For kinetic analysis, it is assumed that the material decomposes according to Eq. (1):

$$\mathrm{A_{solid}} \rightarrow \mathrm{B_{solid\ or\ liquid}} + \mathrm{C_{gas}} \qquad (1)$$

The rate expression d*e*/d*t*, where *e* is the concentration of educt (reactant), is assumed to be defined by Eq. (2):

$$\frac{\mathrm{de}}{\mathrm{dt}} = \mathrm{k(T)} \times \mathrm{f(e,p)} \qquad (2)$$

Where k is the kinetic constant, p is the concentration of the product, $k = A\exp(-E/RT)$ according to the Arrhenius law, A is the frequency factor, E is the activation energy and f(*e,p*) is the so-called ‘‘reaction equation’’ or in the case of TGA, the ‘‘reaction model”.

All reactions are assumed to be irreversible. In the case of degradation and since the evolved gases are continuously removed by the fluid flow in the TGA chamber, this is a reasonable assumption. It is also assumed that the overall reaction (Eq. (9)) is the sum of individual reaction stages (formal or true stage) with constant activation energy, as generally accepted in chemistry. The model can then include competitive, independent and successive reactions. The equations are solved with multivariate kinetic analysis (determination of the parameter via a hybrid normalized Gauss-Newton method or Marquardt method)[4].

By optimizing the models used for the kinetic analysis, the kinetic parameters of each stage in the thermal decomposition model of the material can be evaluated, allowing for a better understanding of the thermal decomposition behavior of the material.

The approach used to model the decomposition behavior of PEEK was similar to that adopted by Moukhina et al, whereby a model free analysis was used to determine the initial kinetic decomposition parameters and gain insight regarding the number of stages involved and the types of kinetic models that govern the decomposition[5]. To this approach, we added our own understanding of the thermal decomposition based our previous work on the same material[2], whereby the thermal decomposition mechanism was attempted.

The reflection behind the methodology that we have adopted is briefly summarized hereunder.

In order to model the kinetic degradation of a polymeric material, two separate functions can be assumed. One being temperature dependent (K(T)), and the other governed by the conversion, α, f(α). The latter can be of any value from 0 (no degradation) to 1 (complete degradation). Therefore, the differential equation that defines the kinetics of thermal degradation can be written as equation 3[6].

$$\frac{d\alpha}{dt} = K(T)f(\alpha) \tag{3}$$

$\frac{d\alpha}{dt}$ is the rate of degradation, K(T) is the temperature dependent rate constant, and $f(\alpha)$ corresponds to the reaction model. $K(T)$ can be described by the Arrhenius equation (equation 4):

$$K(T) = Ae^{-\left(\frac{E}{RT}\right)} \tag{4}$$

Where R is the universal gas constant, E, the activation energy, and A, the pre-exponential factor[7].

The time dependence of equation (4) can be eliminated by using a constant heating rate $\beta = \frac{dT}{dt}$, by dividing by it (equation 5).

$$\frac{d\alpha}{dT} = \frac{A}{\beta} f(\alpha) e^{-\frac{E}{RT}} \quad (5)$$

Linearizing equation 5 leads to obtainable kinetic parameters (A and E) by using the equation 6.

$$\ln\left(\frac{\frac{d\alpha}{dT}}{f(\alpha)}\right) = \ln\left(\frac{A}{\beta}\right) - \left(\frac{E}{RT}\right) \quad (6)$$

One approach for kinetic modelling involved the assumption that the activation energy and the preexponential factor are constant. A well-known technique that uses this method is the Friedman method, whereby the activation energy and pre-exponential factor are obtained by plotting the logarithmic form of the rate equation of each heating rate (equation 3). *α* represents the value at a certain degree of conversion, and *i* the data from the corresponding heating rate experiment[8].

$$\ln\left[\beta_i \left(\frac{d\alpha}{dT}\right)_{\alpha,i}\right] = \ln\left(A_\alpha f(\alpha)\right) - \frac{E_\alpha}{RT_{\alpha,i}}) \quad (7)$$

The activation energy at particular conversion degrees can be calculated with linear regression from a plot of $\ln\left[\beta_i \left(\frac{d\alpha}{dT}\right)_{\alpha,i}\right]$ against $\frac{1}{T_{\alpha,i}}$ for the heating rates that were used. The plot can provide confirmation as to whether there is more than one stage involved in the degradation process. Moreover, the nature of the decomposition stage can also be deduced by comparing the slope of a constant heating rate data[9]. By comparing the magnitudes at the peak slope (the one that is on the right side of the peak) and that of isoconversion lines, three types of reactions are defined: normal, accelerated, and retarded (**Figure 2**).

Figure 2. Friedman plots corresponding to a normal type of reaction (left), an accelerated reaction (middle), and a retarded reaction (right).[9]

A normal reaction corresponds to the curve whereby the magnitude of the peak slope (slope to the right of the peak) and that of the isoconversion lines are of the same magnitude. An accelerated reaction is one whereby the peak slope is steeper than that of the isoconversion lines. Contrarily, a retarded reaction has a peak slope which is gentler than that of the isoconversion lines. However, one of the major limitations of this method is that it does not cater for the possibility of competitive parallel reactions that may occur during the thermal decomposition process.

It should be noted that for the reaction model to make physical sense, reaction orders above three are not considered. However, because of the complexity of the reactions occurring during the thermal decomposition of a polymeric material, optimizations based on experimental data can lead to non-integer values of reaction orders. This often happens when a stage involves more than one pathway towards the same decomposition product.

Another similar method that is used for model free analyses of kinetic degradation is the Ozawa-Flynn-Wall integral isoconversional method[10,11].

The Ozawa-Flynn-Wall analysis involves an integral method for the calculation of the kinetic parameters, therefore, there is no separation of variables involved. As a result, competitive reactions show variations in activation energies between the Ozawa-Flynn-Wall and the Friedman analyses[9]. This will be helpful in determining the nature of the stages involved in the thermal decomposition of the materials investigated.

Moreover, the insight regarding the thermal decomposition behavior of the polymeric materials will be used in order to devise an experiment-based model, aided by the model free analysis detailed above.

There are several reaction types that can be attributed to a decomposition stage. The typical homogenous reactions and classic solid reactions are listed in **Table 1**.

The models were optimized using the KineticsNeo software (Netzsch). We have attempted to make kinetic models with the lowest number of stages that gave an acceptable fit and that were consistent with the thermal decomposition mechanism of the material studied.

Table 1. Reaction types and corresponding reaction equations $\frac{d\alpha}{dt} = -A\, e^{\frac{E}{RT}} f(\alpha)$

3. Results and Discussion

3.1. PI decomposition in nitrogen

TG curves and their corresponding DTG curves when PI is subjected to four different heating rates under nitrogen are shown on **Figure 3**.

Figure 3. TGA (left) and the corresponding DTG (right) curve of PI at 1 (black), 2 (red), 5 (blue), and 10 K/min (magenta), under nitrogen.

From the TGA plots of PI (**Figure 3**), it is clear that PI has a high thermal stability as hardly any mass loss is recorded until almost 500 °C. he temperature at the onset of the decomposition increases with increasing heating rate. It involves an apparent sharp decomposition stage, whereby around 30 wt% of mass loss is observed. This decomposition can be seen as the first peak on the DTG curve. After this peak, the

mass loss rate decreases, but only to around 0.5 wt%/°C. This suggests that there is another stage involved in the thermal decomposition of PI.

It can be noted that the maximum mass loss rate decreases with increasing heating rate. This suggests that the first decomposition stage follows the same kinetic pathway. To further the understanding of the kinetics of the thermal decomposition behavior, the model free analysis (Friedman analysis) was performed on the TGA curves of PI at the different heating rates. The Friedman plot as well as the isoconversion lines corresponding to different conversions are plotted on **Figure 4**.

Figure 4. Friedman analysis of PI using 4 different heating rates under nitrogen (orange: 1 K/min, green: 2 K/min, red: 5 K/min, blue: 10 K/min)

From the Friedman analysis (**Figure 4**), it can be observed that the isoconversion lines to the right of the first peak has a gentler slope than the slope of the peaks. This means that the first decomposition reaction is accelerated. This is often the case in polymeric materials because their decomposition leads to the generation of radicals which are very reactive and contribute to the further decomposition of the material. For this reason, the first stage of the thermal decomposition was assigned to an autocatalytic decomposition rate model (Cn).

Moreover, the activation energy and pre-exponential factor based on the model free Friedman analysis is shown on **Figure 5**.

Figure 5. Activation energy plot for PI under nitrogen, obtained by Friedman analysis

From the two plots on **Figure 5**, it can be seen that the activation energy and the pre-exponential factor are relatively constant at the beginning of the decomposition process, until around 60% of conversion. After this, the activation energy increases rapidly from around 300 to around 1400 kJ/mol at 100% conversion. This means that there are at least two stages in the thermal decomposition of PI under nitrogen. Moreover, at around 90% conversion, there seems to be a slight change in the continuity of the curve, suggesting that there might be another step in the decomposition reaction. In order to check whether there are any competitive reactions occurring, the activation energies calculated from an Ozawa-Flynn-Wall curve was plotted on the same axes as the activation energies from the Friedman plot. This graph is shown on **Figure 6**.

Figure 6. Activation energies calculated using Friedman analysis (black) and the Ozawa-Flynn-Wall method (magenta) for PI under nitrogen

By comparing the evolution of the activation energies calculated from the two aforementioned methods, it can be seen that for the first 50% of the conversion, there is very little difference in activation energy. This means that there are not

competitive reactions in the first step of the thermal decomposition. However, at higher conversions, we can see that the activation energies curves do not have the exact same shape, but the values are only slightly different.

From the model free analyses, we have seen that there are at least three stages in the thermal decomposition of PI under nitrogen. Additionally, the comparison of the activation energies from the derivative model free analysis (Friedman) and the integral model free analysis (Ozawa-Flynn-Wall), we have deduced that there are not competitive reactions occurring during the thermal decomposition. Moreover, it was seen from both the activation energy plots that towards the end of the conversion, the activation energy of the thermal decomposition increases greatly.

These inputs are essential for the elaboration of a kinetic model for the thermal decomposition mechanism of PI. The model that was chosen is illustrated on **Scheme 1** and explained in the subsequent paragraphs.

Scheme 1. Kinetic model used to model the thermal decomposition kinetics of PI under nitrogen

Moreover, in the mechanism of the thermal decomposition of PI that was detailed in our previous work[2], the different reactions occurring during the thermal breakdown of PI under nitrogen are also known. The first stage of the decomposition involves the random scission of the polymer chain. This corresponds to the first decomposition stage, which is also the main decomposition stage of the thermal decomposition. The kinetic model that was used for this stage of the decomposition corresponds to an autocatalytic reaction. Indeed, the random scission of a polymeric chain leads to the formation of reactive radicals that often take part in the subsequent decomposition of a material.

After the random scission of the polymeric chains, small amounts of gases such as ammonia, hydrogen cyanide, and methane gave off and were characterized by TGA connected to Fourier Transform Infrared (FTIR). The formation of methane and hydrogen cyanide probably comes from the secondary decomposition of aromatics that are formed during the char formation process. Indeed, at high temperatures, the char continues to strengthen and degrade, releasing hydrogen and low molecular weight products such as methane. This corresponds to part of the second stage of the decomposition of PI under nitrogen.

Furthermore, the presence of hydrogen (which is assumed by the presence of methane), means that nitrogen containing moieties may be reduced to ammonia at high temperatures. This explains the slightly delayed detection of ammonia in the TGA-FTIR [2], and corresponds to the third stage. **Table 2** shows the kinetic parameters that were optimized for the decomposition model.

Table 2. Kinetic parameters used in the model for the thermal decomposition of PI under nitrogen

The last two stages correspond to extremely high activation energies, which is coherent with both the Friedman and the Ozawa-Flynn-Wall methods. However, the exact reactions occurring at such high temperatures are unknown. This is because the exact structure of the char formed during the initial decomposition is not perfectly known. However, we can safely mention that the 3-stage reaction is coherent with the release of the decomposition products that were identified.

The first stage of the decomposition was assigned to an autocatalytic decomposition, with an activation energy around 278 kJ/mol, a reaction order of 3.00 and an autocatalytic order of 0.377. This activation energy is coherent with the Friedman analysis **Figure 5**. The two subsequent reactions were modeled as Arrhenius reactions, with activation energies of 370 and 410 kJ/mol, respectively. This corresponds to the high activation energy seen for the decomposition at conversions superior to 60%. These two reactions correspond to the slow decomposition of the char formed during the first stage of the decomposition and each share around 20% of contribution to the whole mechanism.

Moreover, from **Table 2**, it can be seen that the first decomposition stage, which corresponds to the autocatalytic stage, is the one that has the highest contribution. The other two stages are also kinetically significant, with contributions of around 19%

From the kinetic parameters in **Table 2**, the best fit model of mass loss with temperature was plotted along with the experimental TGA curves. The resulting graph is shown on

Figure 7.

Figure 7. Best fit of the TG data for the three-stage reaction models in **Scheme 1**, with the parameters given on **Scheme 1**. The curves represent the experimental data and the symbols represent the model

From a statistical point of view, the correlation coefficient of the model with respect to the experimental data was 0.99964.

From the model that was adopted, the major decomposition reaction corresponds to the first stage, with a contribution of 62.5 % in the model. However, the subsequent stages have a non-negligible contribution (18.8 %) to the model. This means that the char decomposition plays a major role in the thermal decomposition model of PI.

Having the kinetics of the decomposition of PI under nitrogen in hand, our interest went to the effect that oxygen may have on kinetics of the thermal decomposition of PI. Therefore, the thermal behavior of PI under 2% oxygen was studied and is detailed in the next section.

3.2. PI decomposition in 2% oxygen

To model the kinetic decomposition of PI under 2% oxygen, dynamic TGA was performed on PI at low oxygen levels at different heating rates. The resulting TG curves and their corresponding DTG curves of PI under 2% oxygen are shown on **Figure 8**.

Figure 8. TGA (left) and the corresponding DTG (right) curve of PI at 1 (black), 2 (red) ,5 (blue), and 10 K/min (magenta), under 2% oxygen

Quite expectedly and similarly to the initial investigation of PI under different oxygen levels, PI remains stable up to a relatively high temperature of around 450 °C. From the TG curves it appears that there is only one decomposition stage in the thermal decomposition of PI under 2% oxygen. Nevertheless, when looking at the DTG curves for heating rates corresponding to 2, 5, and 10 K/min, there seems to be at least two peaks for the thermal decomposition of PI. The absence of a visible second peak at the heating rate of 1K/min is assigned to the two decomposition stages occurring at similar temperature ranges.

Therefore, from the TGA and DTG curves, we can deduce that the thermal decomposition mechanism of PI is at least a two-stage process. To confirm this, Friedman analysis was performed on the data from the above TG curves. The resulting plot is shown in **Figure 9**.

Figure 9. Friedman analysis of PI using 4 different heating rates under 2% oxygen (orange: 1 K/min, green: 2 K/min, red: 5 K/min, blue: 10 K/min)

The Friedman plot shows a small peak at the beginning of the decomposition, followed by another at around 50% conversion. Finally, another decomposition stage is visible towards 100% conversion. This peak is not visible in the Friedman plot at 10 K/min. This may be because at the maximum temperature of the TG experiment, the mass loss was not total, suggesting that the reaction had not reached its completion. From these plots, we can deduce that there are at least three stages involved in the thermal decomposition of PI under 2% oxygen.

From this Friedman plot, the activation energies as well as the pre-exponential factor for the decomposition of PI was plotted with respect to the conversion (**Figure 10**). This is essential to obtain initial parameters for the modeling of the thermal decomposition of PI.

Figure 10. Activation energy plot for PI under 2% oxygen, obtained by Friedman analysis

From this Friedman plot, it can be seen that at low conversion, the activation energy is relatively high (around 350 kJ/mol). This corresponds to the first stage of the decomposition. However, as the material decomposes further, the activation energy decreases rapidly and is dependent on the conversion degree. This is assigned to the second stage of the thermal decomposition. At conversions above 70%, the

activation energy is still dependent on the conversion, but unlike the previous stage, it seems to increase slightly. This is assigned to the third stage of the decomposition.

Based on the two Friedman analysis plots, we have seen that the thermal decomposition of PI under 2% oxygen corresponds to at least three stages of decomposition. In order to have insight concerning eventual competitive reactions that might be occurring during the decomposition of PI, the activation energy based on calculations using Friedman analysis was compared to that based on the OFW method (**Figure 11**). Because of the difference in the approach for the two similar methods, the occurrence of competitive reactions is translated by a difference in activation energy for the same conversion.

Figure 11. Activation energies calculated using Friedman analysis (black) and the Ozawa-Flynn-Wall method (magenta) for PI under 2% oxygen

From the two activation energy plots, it can be seen that the global shapes of the two activation energy plots are relatively similar. Indeed, the activation energy increases for early conversions and then decreases. The increase in activation energy can be assigned to the breaking of chemical bonds (endothermic) which generate radicals. The following decrease in activation energy is assigned to recombination reactions between radicals which potentially lead to the formation of a stable char (exothermic).

Moreover, there is a slight difference in the activation energy for the first stage of decomposition. However, the error is significant for the first stage of the decomposition. It is therefore hard to conclude whether the competitive stage occurs during the first stage or later. As a result, the kinetic decomposition model was based on the understanding of chemical reactions occurring at the onset of the decomposition.

The model free analyses have provided insight on the number of stages that are involved in the thermal decomposition of PI. Using knowledge acquired from the thermal decomposition of PI in our previous work[2], kinetic model for the thermal decomposition of PI under 2% oxygen is suggested (Scheme 2).

Scheme 2. Kinetic model used to model the thermal decomposition kinetics of PI under 2% oxygen

Similarly to the decomposition of PI under nitrogen, a three-stage pathway was used to model the thermal decomposition of PI under 2% oxygen. However, in order to involve the thermo-oxidation reactions in the model, a supplementary stage was required. From the TGA of PI under varying oxygen concentrations[2], it was seen that oxygen intervenes right at the start of the decomposition. Therefore, the thermo-

oxidation stage was added as a competitive reaction at the very first stage of the decomposition model (stage 1.2).

The optimized kinetic parameters for the thermal decomposition of PI under 2% oxygen are summarized in **Table 3**.

Table 3. Kinetic parameters used in the model for the thermal decomposition of PI under 2 % oxygen

The optimized parameters for the kinetic model fit well with the experimental TG curves (**Figure 12**). The activation energy for the two competitive reactions at the beginning of the reaction are of the same order of magnitude. One of the two reactions from the first stage of the decomposition is assigned to the thermal decomposition of PI, while the other one is assigned to the thermo-oxidation of the polymer backbone.

Since thermo-oxidation usually results in the formation of carbon dioxide, carbon monoxide and water, no subsequent reaction is assigned after the reaction corresponding to the thermo-oxidation of the polymer backbone.

The second stage is assigned to the subsequent thermal decomposition of the decomposition products formed during the initial thermal decomposition. Indeed, from the previous study, we have concluded that the first decomposition of PI may lead to the formation of a thermally stable char, or another crosslinked structure.

The formation of this structure is aided by the presence of radicals resulting from the initial decomposition reactions (stage 1.1). Moreover, this structure may further thermally decompose into smaller structures. This leads to the formation of more radicals that can in turn participate in furthering the decomposition. Therefore, the second stage of the decomposition of PI was assigned to an autocatalytic reaction type. This stage has a relatively low activation energy because of the presence of radicals that are still lingering around the polymer after the first decomposition stage. Moreover, these recombination reactions eventually lead to stable char formation as it was seen in our previous work dealing with the decomposition mechanism of PI.[12] Char formation reactions are exothermic and could also explain the lowering of the activation energy on the activation energy plot on **Figure 10**.[13]

The last reaction stage corresponds to the thermo-oxidation of the remaining organic material and carbonaceous char.

Figure 12. Best fit of the TG data for the three-stage reaction models in **Scheme 2**, with the parameters given on **Table 3**. The curves represent the experimental data and the symbols represent the model.

When comparing with the decomposition model under nitrogen, an additional competitive decomposition reaction is observed in the first stage of the thermal decomposition model of PI under low oxygen concentration. This is because thermo-

oxidation occurs right at the beginning of the decomposition of PI, parallelly to pyrolytic decomposition. It is interesting to note that these two initial decomposition reactions have a significant contribution to the decomposition. Indeed, about 50 % of the model is assigned to the two initial stages. The other decomposition stages correspond to the char degradation and oxidation. Moreover, from a statistical point of view, the correlation coefficient between the experimental curve and the simulated curve based on the kinetic model is 0.99949., meaning that the model used to simulate the thermal decomposition of PI under 2% oxygen is consistent with the experimental TG curves.

To complete the investigation of the kinetics of the thermal decomposition of PI under different oxygen concentrations, the behavior of PI in air was also investigated.

3.3. PI decomposition in air

After having investigated the thermal decomposition behavior of PI under low oxygen concentrations the kinetic of the thermal decomposition of PI in air was studied so that the effect of a highly thermo-oxidative atmosphere can be better understood. This also allows for the simulation of the degradation behavior when the material is subjected to heat in a well-ventilated environment. The presence of oxygen in air usually increases the extent to which a material decomposes when under thermal stress. Sometimes, oxygen can have a catalytic effect on the onset of the decomposition of a material.

Dynamic TGA was used to investigate the kinetics of the thermal decomposition behavior of PI in air. The TG curves of PI and their corresponding DTG curves at four different heating rates are shown on **Figure 13**.

Figure 13. TGA (left) and the corresponding DTG (right) curve of PI at 1 (black), 2 (red) ,5 (blue), and 10 K/min (magenta), in air.

From the TG curves of PI in air, it can be seen that the thermal stability of PI is maintained until around 450 °C, whereby the onset of thermal decomposition is observed at the beginning of a mass loss process. The TG curves all appear to follow an apparent single stage. However, on the DTG curves, at high heating rates, a second peak, which is close to the first, is noticeable. This means that the kinetics of the thermal decomposition of PI in air occurs in at least two stages. In order to obtain further information regarding the number of stages and the types of reactions occurring during the thermo-oxidative decomposition of PI in air, the Friedman plot for the corresponding heating rates was plotted (**Figure 14**).

Figure 14. Friedman analysis of PI using 4 different heating rates in air (orange: 1 K/min, green: 2 K/min, red: 5 K/min, blue: 10 K/min)

From the Friedman plot, an accelerated decomposition stage can be distinguished as a first peak. The peak slope is steeper than the isoconversion lines. This suggests that the first decomposition stage is accelerated, probably autocatalytic[9]. At higher heating rates (5 and 10 K/min) there seems to be another peak that is visible right after the first one. This confirms that there are at least two stages in the thermal decomposition of PI in air. it is therefore likely that at low heating rates, the two thermal decomposition stages are overlapping.

In order to see any eventual reactions that may be occurring during the thermo-oxidative decomposition of PI, the activation energy and log(pre-exponential factor) (calculated from the Friedman analysis), was plotted with respect to the conversion (**Figure 15**).

Figure 15. Activation energy plot for PI in air, obtained by Friedman analysis

The activation energy is relatively high at the beginning of the conversion (around 190 kJ/mol). It decreases until around 60% conversion where the activation energy is at around 130 kJ/mol. This means that there is another stage in the decomposition of PI. At this point, and until almost 98 % conversion, there is little evolution in the activation energy. At 100% conversion, there is a high increase in activation energy. However, the error at this conversion is very high, therefore, it was not taken into consideration as a subsequent decomposition stage.

The activation energy plot based on the Friedman method provided out the number of consecutive stages occurring during the thermo-oxidative decomposition of the material. To further the understanding of decomposition in terms of competitive reactions that may occur, the activation energy plot based on the Friedman method was compared with that based on the OFW method (**Figure 16**).

Figure 16. Activation energies calculated using Friedman analysis (black) and the Ozawa-Flynn-Wall method (magenta) for PI in air.

From the two activation energy plots on **Figure 16**, it can be seen that the two methods lead to very different activation energies in at around 50% conversion. This strongly suggests that there are competitive reactions occurring during the thermal decomposition of PI in air. It was therefore considered when elaborating the kinetic model for the thermo-oxidative decomposition of PI.

Based on knowledge acquired during the investigation of the thermal stability of PI and its thermal decomposition mechanism under nitrogen, we were able to take an attempt at defining a kinetic model for the thermo-oxidative decomposition of PI in air. The model is shown on **Scheme 3**.

Scheme 3. Kinetic model used to model the thermal decomposition kinetics of PI in air.

From **Scheme 3**, two major consecutive decomposition stages are illustrated. The first corresponds to the initial decomposition of PI, similarly to the thermal decomposition of PI under nitrogen. It corresponds to the random scission of the polymer backbone. However, it was observed that the presence of oxygen tends to slightly decrease the thermal stability of PI at high temperatures[2]. This translates into a lower activation energy for the onset of the decomposition. Additionally, the initial decomposition leads to the formation of reactive radicals which can take part in the scission of the initial polymer. This effect can be assigned to an autocatalytic type of decomposition reaction whereby the products increase the rate of the decomposition. During this stage, rearrangement of the polymer backbone to form a crosslinked char structure was also hypothesized under nitrogen. This char is highly stable under inert atmosphere, but not under oxygen. This was evidenced by the TGA under different oxygen levels, whereby the second decomposition of PI was largely affected by the presence of oxygen.

It was therefore not unexpected to add a stage whereby the thermo-oxidative reactions are occurring. This corresponds to stage 2.2. Furthermore, while the material is being thermo-oxidized, there are also thermal decomposition that is on-going, via a similar mechanism as the first stage. However, the initial structure of the polymer has changed, and so have the kinetic parameters for the decomposition stage. Therefore, an autocatalytic type decomposition mechanism was assigned to this stage.

The optimized kinetic parameters used in for the modeling of the thermal decomposition of PI in air are summarized in **Table 4**.

Table 4. Kinetic parameters used in the model for the thermal decomposition of PI in air

The activation energy for the first decomposition stage is coherent with the activation energy calculated using the Friedman analysis for the first stage (**Figure 15**). This first stage of thermal decomposition formed a charred structure and possibly a partially decomposed form of the polymer. Further thermal decomposition of this structure is modeled by reaction 2.1. This was assigned to a similar reaction as the first decomposition stage. However, since the chains have already partially been broken, the activation energy is lower. Moreover, in the presence of air, the structure undergoes thermo-oxidation (modeled by reaction 2.2).

The simulated TG curves based on the kinetic model above as well as the experimental TG curves are shown on **Figure 17**.

Figure 17. Best fit of the TG data for the three-stage reaction models in **Scheme 3**, with the parameters given on **Table 4**. The curves represent the experimental data and the symbols represent the model.

Contrarily to the kinetic model of the thermal decomposition of PI under 2% oxygen, the model in air does not have competitive reactions in the initial decomposition stage. However, the autocatalytic nature of the reaction model suggests that there are reactive decomposition products that are released during that stage, leading to the formation of a char as well as releasing oxidation products. Moreover, the other two decomposition reactions have been assigned to two thermo-oxidation reactions, each with a significant contribution as compared to the first stage of the decomposition. Indeed, the decomposition of the char (stage 2.2) and the further thermo-oxidation of the polymer (stage 2.1) play a bigger role in the thermal decomposition than the initial char formation reaction (stage 1). It is interesting to note that the thermo-oxidation of the char corresponds to a low order kinetic reaction model (reaction order = 0.06). This means that it is only slightly dependent on the "concentration" of the reactants.

The fitted curve seems to correspond well with the experimental curve. From a statistical point of view, the correlation coefficient between the experimental and the simulated curve is 0.99993.

4. Discussion and Conclusion

The kinetic parameters for the thermal decomposition of PI under three different oxygen levels have been calculated. We have seen that, from a kinetic perspective, the decomposition pathway adopted by PI during its thermal decomposition is significantly dependent on the oxygen concentration.

Under nitrogen, the kinetic pathway adopted during its thermal decomposition is relatively simple. However, the presence of a small amount of oxygen brings about a significant change in kinetic pathway adopted by the material during its thermal decomposition. Indeed, in the presence of a small concentration of oxygen, the decomposition pathway is much complexified, leading to a 3-stage decomposition involving a competitive reaction at the initial decomposition stage. Moreover, it was reported that the presence of oxygen increases the crosslinking that occurs in a material [14]. This can be extrapolated to PI, which is also a highly charring polymeric material. Therefore, the higher activation energy that is observed for the thermal decomposition of PI under low oxygen concentration suggests that major crosslinking would have had occurred during the initial decomposition reactions.

Under air, the activation energy for the onset of the decomposition is lower than under pyrolytic conditions. One explanation for this can be that decomposition gases that are produced at the beginning of the decomposition are readily oxidized. A fast consumption of the decomposition gases pulls the kinetics towards the further decomposition of the material. Moreover, the presence of recombination reactions within the polymeric matrix may also be occurring owing to the charring properties of

the polymer can also explain the lowered activation energy due to their exothermic nature.

We have seen that from a kinetics perspective, the pathway adopted by PI during its thermal decomposition is highly dependent on the oxygen concentration. Moreover, low oxygen concentration leads to a higher crosslinking, leading to an increase in the activation energy of the onset of decomposition. However, in air, the crosslinking is taken over (for the most part), by thermo-oxidation. The difference in the kinetics of the thermal decomposition of PI has provided deep insight on the eventual behavior of the material under a fire scenario.

Funding: This work has received funding from the European Research Council's under the European Union's H2020 – the Framework programme for Research and Innovation (2014 – 2020) / ERC Grant Agreement No. 670747 – ERC 2014 AdG/FireBar-Concept

Conflicts of Interest: The authors declare no conflict of interest.

5. References

1. Ramgobin A, Fontaine G, Bourbigot S. Thermal Degradation and Fire Behavior of High Performance Polymers. *Polym Rev*. 2019;59(1):55-123. doi:10.1080/15583724.2018.1546736

2. Ramgobin A, Fontaine G, Bourbigot S. Investigation of the thermal stability and fire behavior of high performance polymer: A case study of polyimide. *Fire Saf J*. 2020;(April):103060. doi:10.1016/j.firesaf.2020.103060

3. Opfermann J. Kinetic analysis using multivariate non-linear regression. I. Basic concepts. *J Therm Anal Calorim*. 2000;60(2):641-658. doi:10.1023/A:1010167626551

4. Kaisersberger E, Opfermann J. Kinetic evaluation of exothermal reactions measured by DSC. *Thermochim Acta*. 1991;187(C):151-158. doi:10.1016/0040-6031(91)87189-4

5. Moukhina E. Determination of kinetic mechanisms for reactions measured with thermoanalytical instruments. *J Therm Anal Calorim*. 2012;109(3):1203-1214. doi:10.1007/s10973-012-2406-3

6. Kinetics SR. Chapter 3 Theory of Solid State Reaction Kinetics. *Compr Chem Kinet*. 1980;22(C):41-113. doi:10.1016/S0069-8040(08)70384-4

7. Vyazovkin S. Kinetic concepts of thermally stimulated reactions in solids: A view from a historical perspective. *Int Rev Phys Chem*. 2000;19(1):45-60. doi:10.1080/014423500229855

8. Friedman HL. Kinetics of Thermal Degradation of Char-Forming Plastics from Thermogravimetry . Application to a Phenolic Plastic. (6):183-195.

9. Hondred PR, Yoon S, Bowler N, Moukhina E, Kessler MR. Degradation kinetics of polyimide film. *High Perform Polym*. 2011;23(4):335-342. doi:10.1177/0954008311409262

10. Ozawa T. A New Method of Analyzing Thermogravimetric Data. *Bull Chem Soc Jpn*. 1965;38(11):1881-1886. doi:10.1246/bcsj.38.1881

11. Flynn JH, Wall LA. A quick, direct method for the determination of activation energy from thermogravimetric data. *J Polym Sci Part B Polym Lett*. 1966;4(5):323-328. doi:10.1002/pol.1966.110040504

12. Ramgobin A, Fontaine G, Bourbigot S. Investigation of the thermal stability and fire behavior of high performance polymer: A case study of polyimide. *Fire Saf J*. 2020;(May). doi:10.1016/j.firesaf.2020.103060

13. Li J, Stoliarov SI. Measurement of kinetics and thermodynamics of the thermal degradation for charring polymers. *Polym Degrad Stab*. 2014;106:2-15. doi:10.1016/j.polymdegradstab.2013.09.022

14. Courvoisier E, Bicaba Y, Colin X. Multi-scale and multi-technique analysis of the thermal degradation of poly(ether ether ketone). *Polym Degrad Stab*. 2018;151(December 2017):65-79. doi:10.1016/j.polymdegradstab.2018.03.001

6. Figures

Figure 1. TG and DTG plots of PI heated at 10 °C/min under nitrogen, 2%, 4%, 8% and 12%, and in air[2].

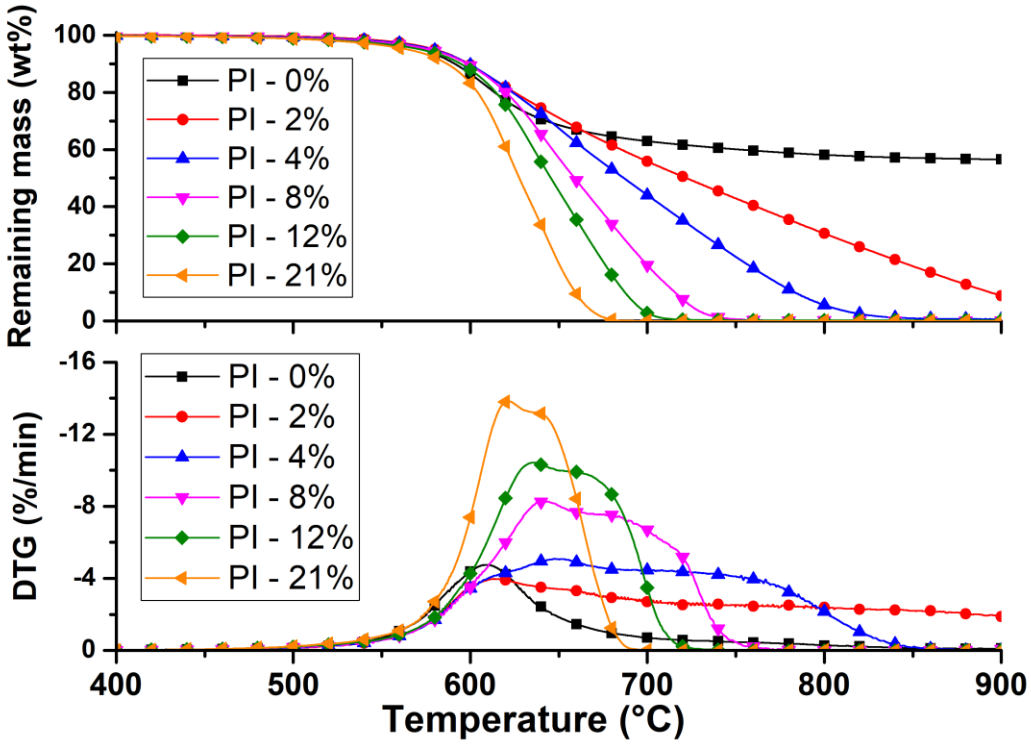

Figure 2. Friedman plots corresponding to a normal type of reaction (left), an accelerated reaction (middle), and a retarded reaction (right).[9]

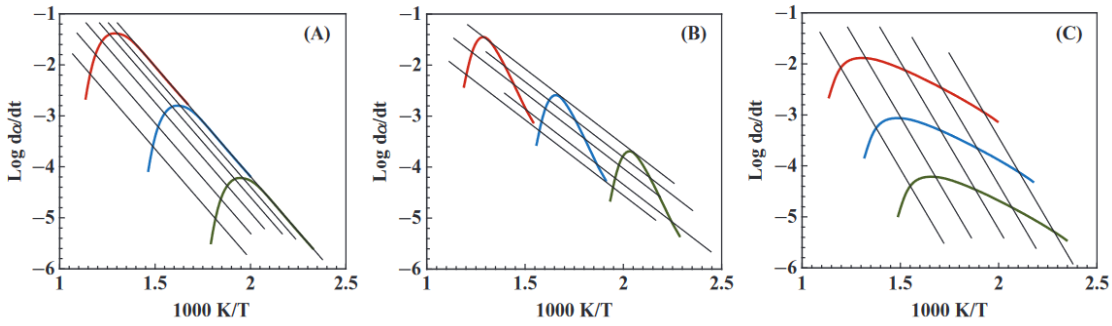

Figure 3. TGA (left) and the corresponding DTG (right) curve of PI at 1 (black), 2 (red), 5 (blue), and 10 K/min (magenta), under nitrogen.

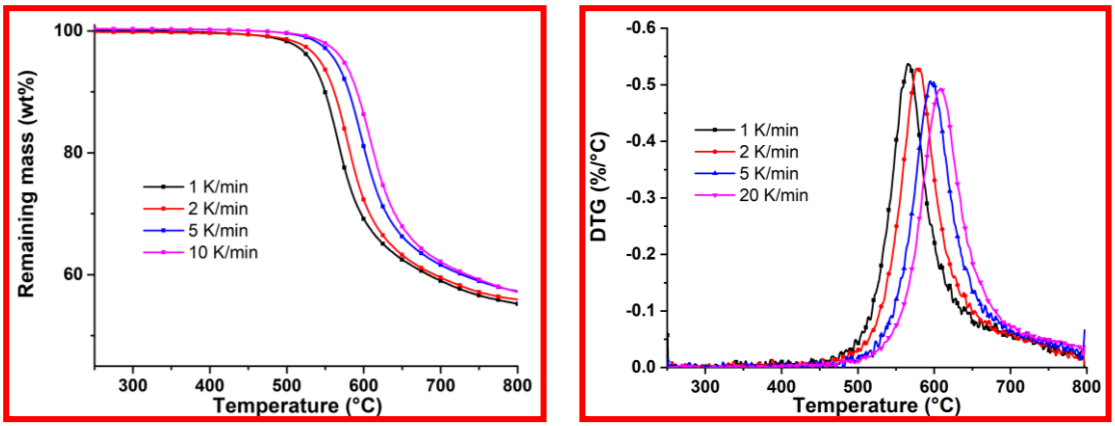

Figure 4. Friedman analysis of PI using 4 different heating rates under nitrogen (orange: 1 K/min, green: 2 K/min, red: 5 K/min, blue: 10 K/min)

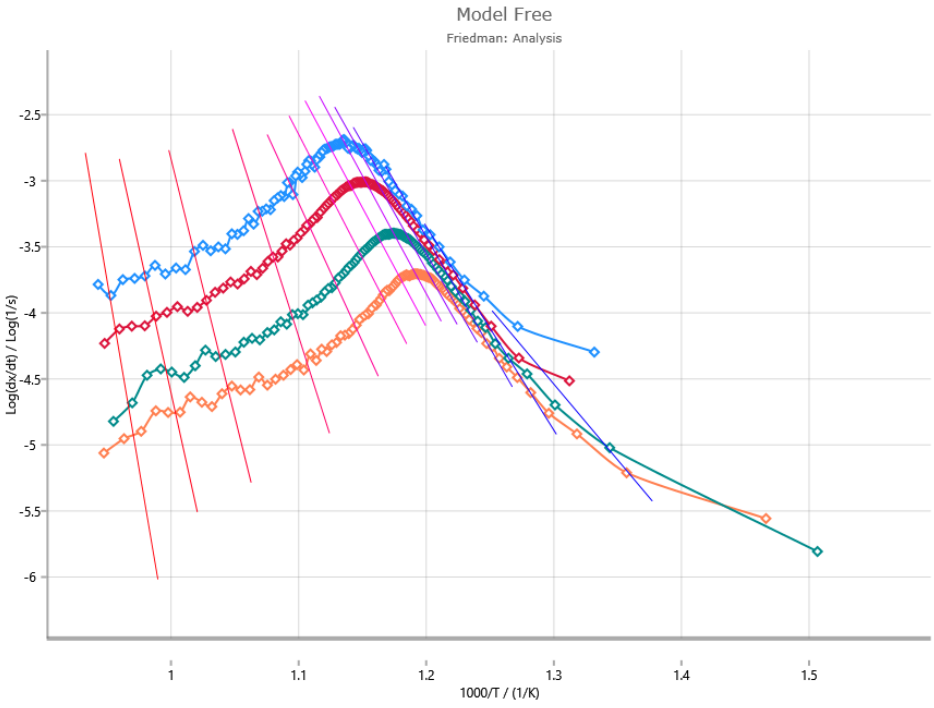

Figure 5. Activation energy plot for PI under nitrogen (left), obtained by Friedman analysis

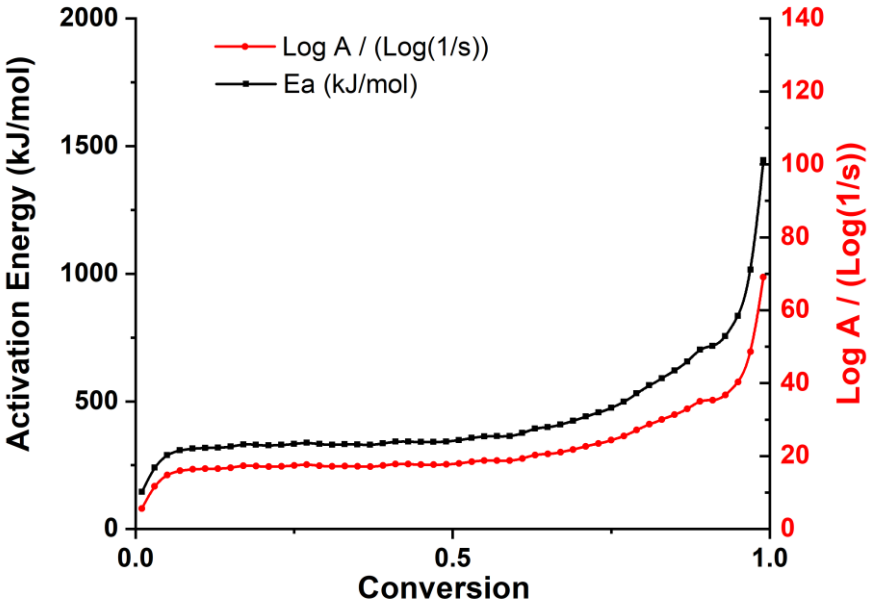

Figure 6. Activation energies calculated using Friedman analysis (black) and the Ozawa-Flynn-Wall method (magenta) for PI under nitrogen

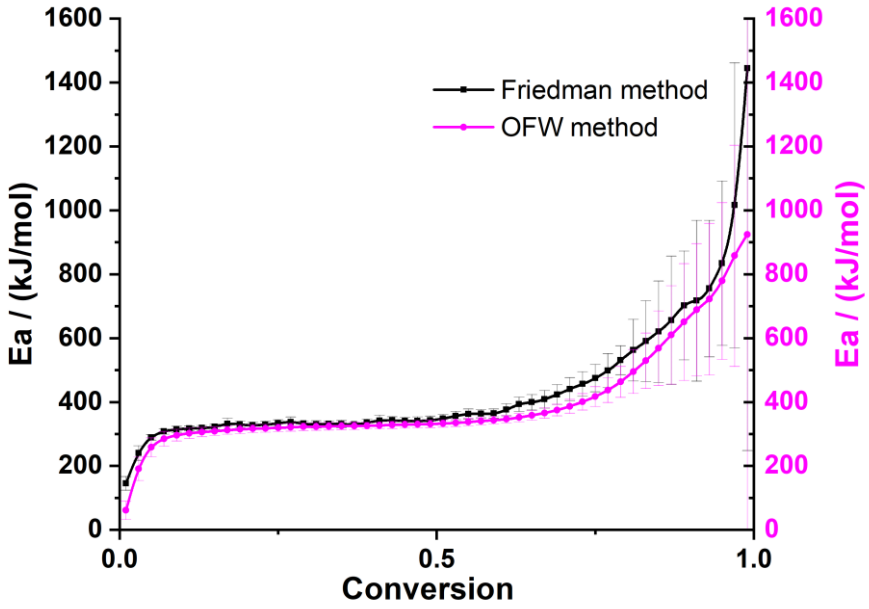

Figure 7. Best fit of the TG data for the three-stage reaction models in **Scheme 1**, with the parameters given on **Scheme 1**. The curves represent the experimental data and the symbols represent the model

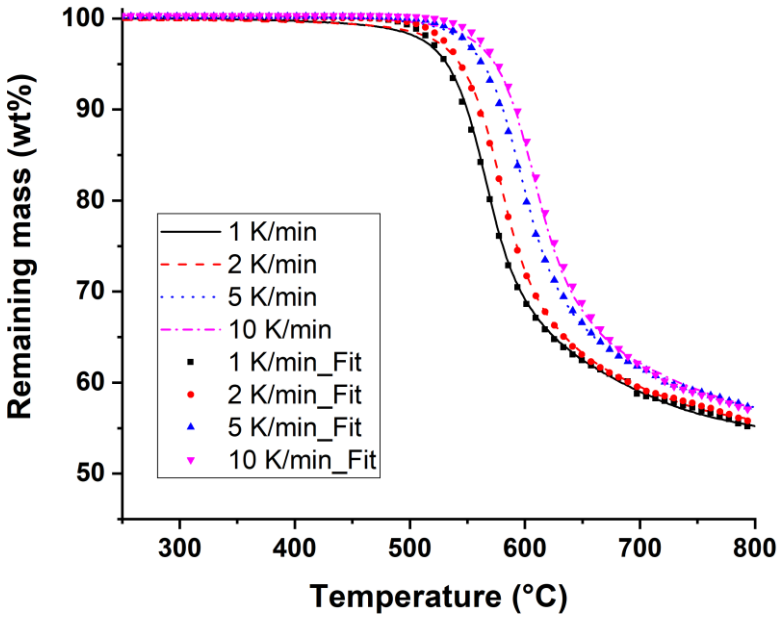

Figure 8. TGA (left) and the corresponding DTG (right) curve of PI at 1 (black), 2 (red) ,5 (blue), and 10 K/min (magenta), under 2% oxygen

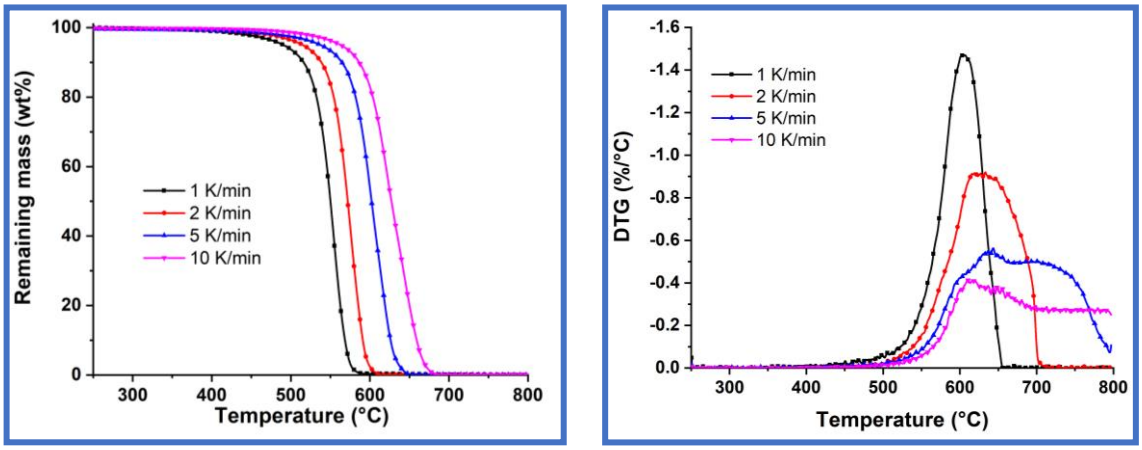

Figure 9. Friedman analysis of PI using 4 different heating rates under 2% oxygen (orange: 1 K/min, green: 2 K/min, red: 5 K/min, blue: 10 K/min)

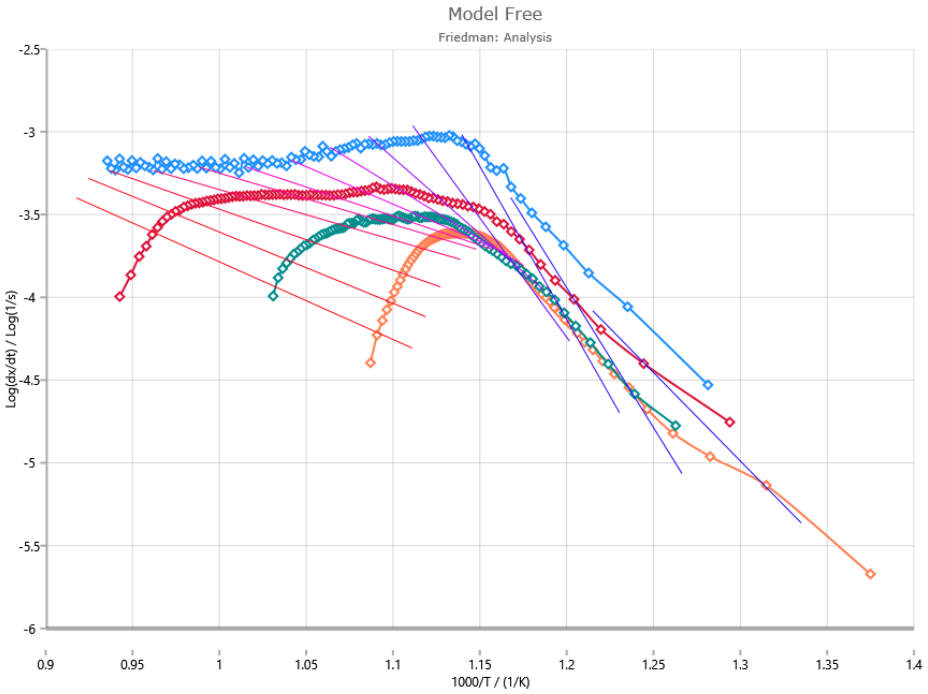

Figure 10. Activation energy plot for PI under 2% oxygen, obtained by Friedman analysis

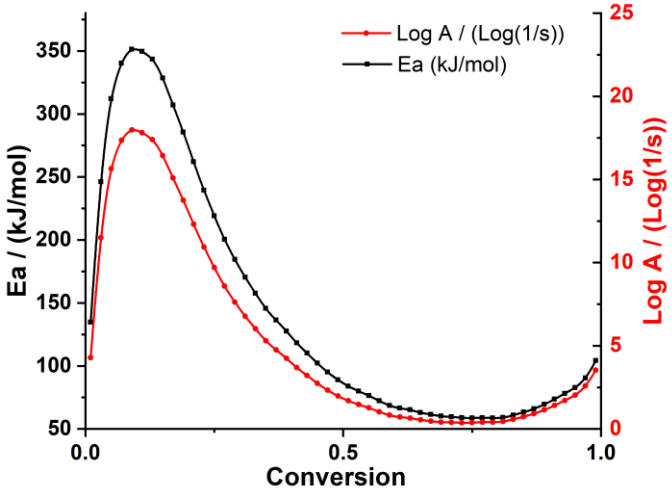

Figure 11. Activation energies calculated using Friedman analysis (black) and the Ozawa-Flynn-Wall method (magenta) for PI under 2% oxygen

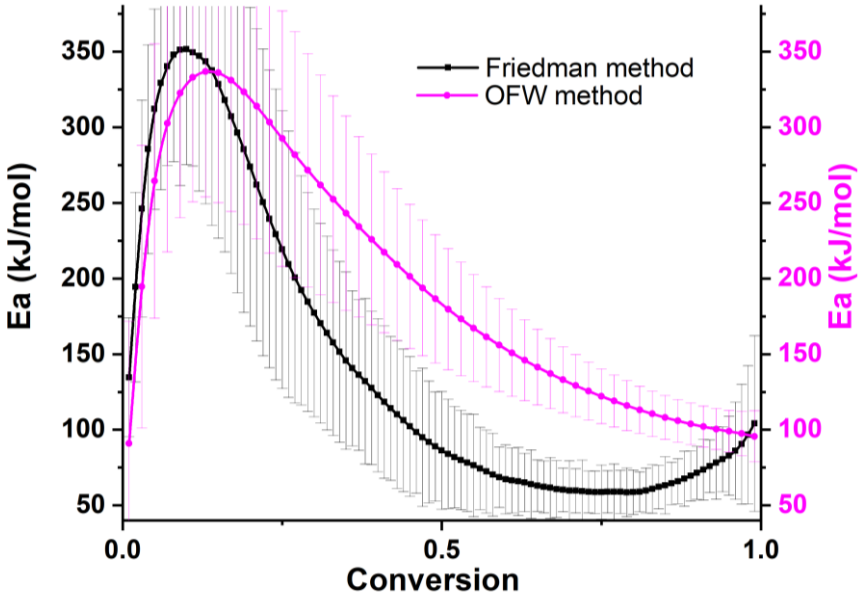

Figure 12. Best fit of the TG data for the three-stage reaction models in **Scheme 2**, with the parameters given on **Table 3**. The curves represent the experimental data and the symbols represent the model.

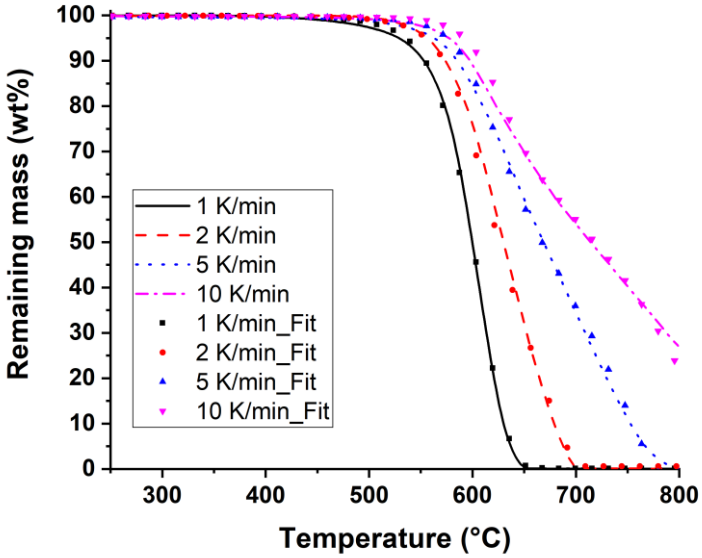

Figure 13. TGA (left) and the corresponding DTG (right) curve of PI at 1 (black), 2 (red) ,5 (blue), and 10 K/min (magenta), in air.

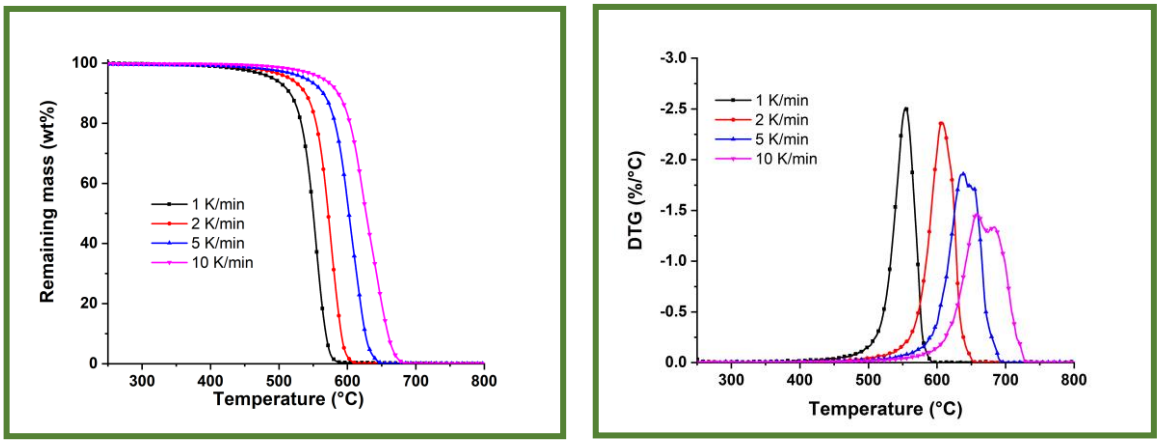

Figure 14. Friedman analysis of PI using 4 different heating rates in air (orange: 1 K/min, green: 2 K/min, red: 5 K/min, blue: 10 K/min)

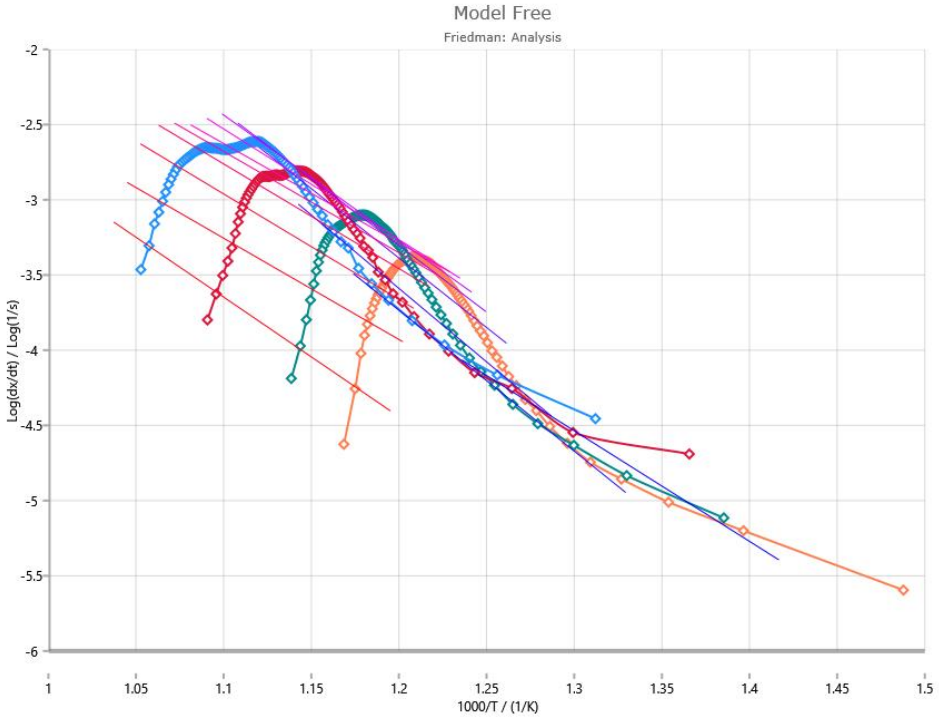

Figure 15. Activation energy plot for PI in air, obtained by Friedman analysis

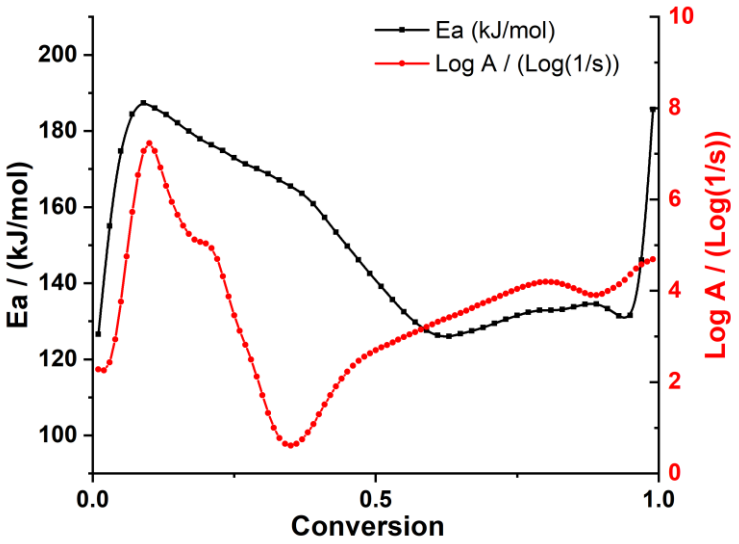

Figure 16. Activation energies calculated using Friedman analysis (black) and the Ozawa-Flynn-Wall method (magenta) for PI in air.

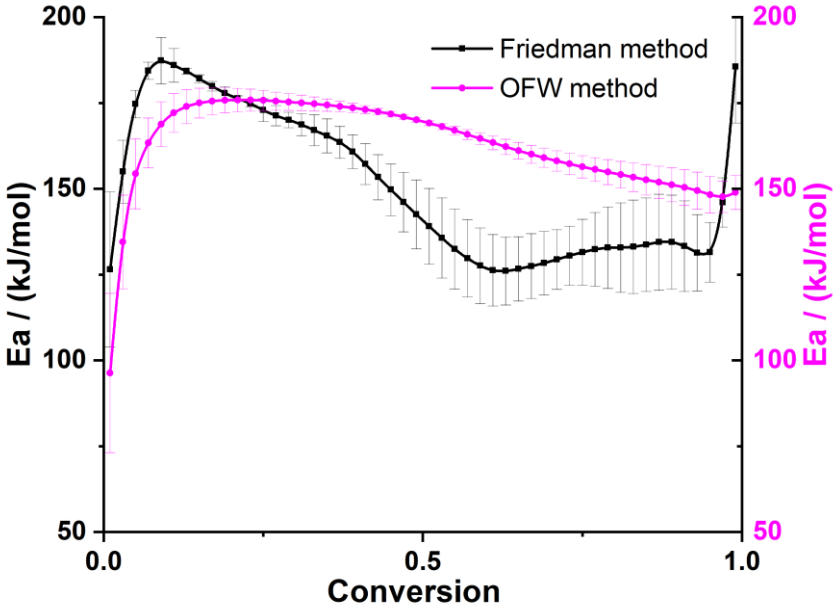

Figure 17. Best fit of the TG data for the three-stage reaction models in **Scheme 3**, with the parameters given on **Table 4**. The curves represent the experimental data and the symbols represent the model.

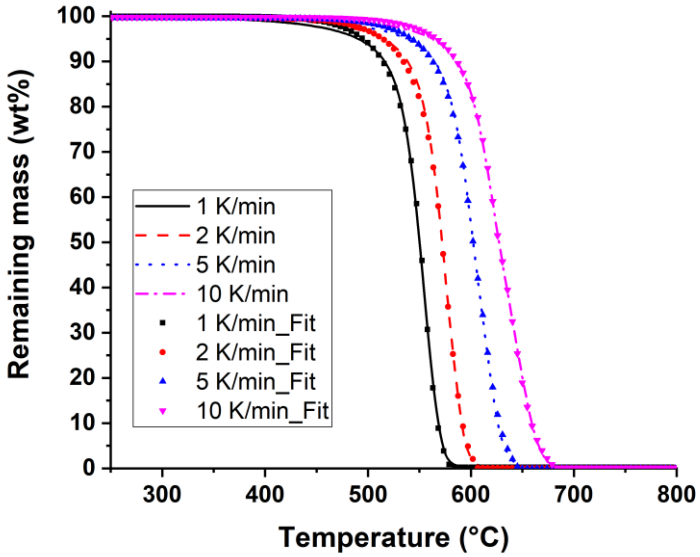

Scheme 1. Kinetic model used to model the thermal decomposition kinetics of PI under nitrogen.

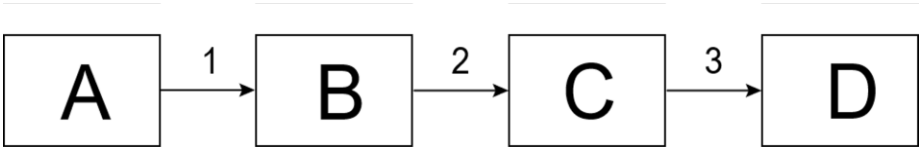

Scheme 2. Kinetic model used to model the thermal decomposition kinetics of PI under 2% oxygen

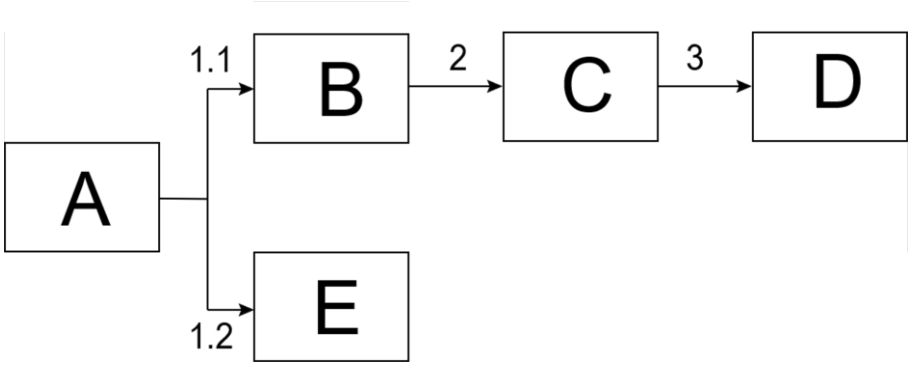

Scheme 3. Kinetic model used to model the thermal decomposition kinetics of PI in air.

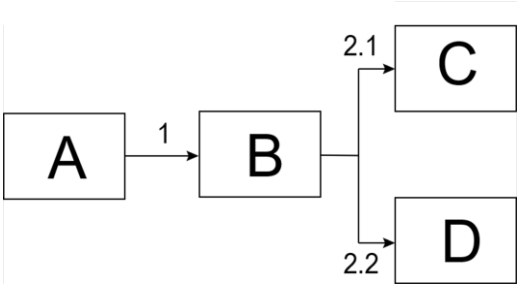

703 **Table 1**. Reaction types and corresponding reaction equations $d\alpha dt = -A\ eERTf(\alpha)$
704

Code	Function	Type of reaction
F1	$f = (1-\alpha)$	Reaction of 1st order
F2	$f = (1-\alpha)^2$	Reaction of 2nd order
Fn	$f = (1-\alpha)^n$	Reaction of nth order
R2	$f = 2(1-\alpha)^{\frac{1}{2}}$	Two-dimensional phase boundary
R3	$f = 3(1-\alpha)^{\frac{2}{3}}$	Three-dimensional phase boundary
D1	$f = \frac{1}{2} \cdot \frac{1}{\alpha}$	One-dimensional diffusion
D2	$f = -\frac{1}{\ln((1-\alpha))}$	Two-dimensional diffusion
D3	$f = \frac{3}{2} \cdot \frac{(1-\alpha)^{\frac{2}{3}}}{1-(1-\alpha)^{\frac{1}{3}}}$	Three-dimensional diffusion Jander's type
D4	$f = \frac{3}{2} \cdot \frac{1}{((1-\alpha)^{-\frac{1}{3}} - 1)}$	Three-dimensional diffusion Ginstling-Brounstein type
B1	$f = (1-\alpha) \cdot \alpha$	Prout-Tompkins equation
Bna	$f = (1-\alpha)^n \cdot \alpha^{K_{cat}}$	Expanded Prout-Tompkins equation
C1	$f = (1-\alpha) \cdot (1 + K_{cat} \cdot \alpha)$	Reaction of 1st order with autocatalysis by product
Cn	$f = (1-\alpha)^n \cdot (1 + K_{cat} \cdot \alpha)$	Reaction of nth order with autocatalysis by product
Cnm	$f = (1-\alpha)\text{^}n \cdot (1 + K_{cat} \cdot \alpha^m)$	Reaction of nth order with m-Power autocatalysis by product
A2	$f = 2(1-\alpha) \cdot [-\ln(1-\alpha)]^{\frac{1}{2}}$	Two-dimensional nucleation according to Avrami
A3	$f = 3(1-\alpha) \cdot [-\ln(e)]^{\frac{2}{3}}$	Three-dimensional nucleation according to Avrami
An	$f = n \cdot (1-\alpha) \cdot [-\ln((1-\alpha))]^{\frac{n-1}{n}}$	n-dimensional nucleation according to Avrami-Erofeev

705

706 **Table 2**. Kinetic parameters used in the model for the thermal decomposition of PI
707 under nitrogen

Stage (reaction type)	1 (Cna)	2 (Fn)	3 (Fn)
Ea (kJ/mol)	277.768	369.820	410.149
Log(A) (log(1/s)	14.351	20.459	23.316
Reaction order	3.000	1.593	1.708
Kcat	0.377	-	-
Contribution	0.625	0.188	0.187

708

709 **Table 3.** Kinetic parameters used in the model for the thermal decomposition of PI
710 under 2 % oxygen

Stage (reaction type)	1.1 (Fn)	1.2 (Fn)	2 (Cn)	3 (Fn)
Ea (kJ/mol)	349	353	62	99
Log(A) (log(1/s)	18.2	17.3	0.1	2.3
Reaction order	1.8	1.1	0.52	0.01
Kcat	-	-	1.69	-
Contribution	0.192	0.290	0.296	0.222

711

712

713

714 **Table 4.** Kinetic parameters used in the model for the thermal decomposition of PI
715 in air
716

Stage (reaction type)	**1 (Cna)**	**2.1 (Cna)**	**2.2 (Fn)**
Ea (kJ/mol)	181	122	112
Log(A) (log(1/s)	7.9	4.2	2.9
Reaction order	0.41	1.24	0.06
Kcat	0.73	0.97	-
Contribution	0.166	0.291	0.543

717